

Determining the sign of the $b \rightarrow s\gamma$ amplitude

Paolo Gambino¹, Ulrich Haisch² and Mikołaj Misiak³

¹ *INFN, Torino and Dip. di Fisica Teorica, Univ. di Torino,
10125 Torino, Italy*

² *Theoretical Physics Department, Fermilab, Batavia, IL 60510, USA*

³ *Institute of Theoretical Physics, Warsaw University,
Hoża 69, PL-00-681 Warsaw, Poland.*

Abstract

The latest Belle and BaBar measurements of the inclusive $\bar{B} \rightarrow X_s l^+ l^-$ branching ratio have smaller errors and lower central values than the previous ones. We point out that these results indicate that the sign of the $b \rightarrow s\gamma$ amplitude is the same as in the SM. This underscores the importance of $\bar{B} \rightarrow X_s l^+ l^-$ in searches for new physics, and may be relevant for neutralino dark matter analyses within the MSSM.

The branching ratio of the inclusive radiative B -decay is one of the most important constraints for a number of new physics models, because it is accurately measured and its theoretical determination is rather clean. The present world average $\mathcal{B}(\bar{B} \rightarrow X_s \gamma) = (3.52 \pm 0.30) \times 10^{-4}$ [1] agrees very well with the Standard Model (SM) prediction $\mathcal{B}(\bar{B} \rightarrow X_s \gamma)_{\text{SM}} = (3.70 \pm 0.30) \times 10^{-4}$ [2]. A well-known way to avoid this constraint without excluding large new physics effects consists in having new physics contributions that approximately reverse the sign of the amplitude $A(b \rightarrow s \gamma)$ with respect to the SM and leave $\mathcal{B}(\bar{B} \rightarrow X_s \gamma)$ unaltered within experimental and theoretical uncertainties. Several authors pointed out that even a rather rough measurement of the inclusive $\bar{B} \rightarrow X_s l^+ l^-$ branching ratio could provide information on the sign of $A(b \rightarrow s \gamma)$ [3].

Other observables that are sensitive to the sign of $A(b \rightarrow s \gamma)$ are the forward-backward and energy asymmetries in inclusive and exclusive $b \rightarrow s l^+ l^-$ decays [3, 4]. Very recently, the first measurement of the forward-backward asymmetry in $B \rightarrow K^{(*)} l^+ l^-$ was announced by the Belle collaboration [5]. Within the limited statistical accuracy, however, the results were found to be consistent with both the SM and the “wrong-sign” $A(b \rightarrow s \gamma)$ case.

The purpose of the present letter is to point out that the present measurements of $\mathcal{B}(\bar{B} \rightarrow X_s l^+ l^-)$ already indicate that the sign of $A(b \rightarrow s \gamma)$ is unlikely to be different from the SM. The experimental results that we consider are summarized in Tab. 1.

	Belle [6]	BaBar [7]	weighted average
$(2m_\mu)^2 < q^2 < (m_B - m_K)^2$	$4.11 \pm 0.83 \begin{smallmatrix} +0.74 \\ -0.70 \end{smallmatrix}$	$5.6 \pm 1.5 \pm 0.6 \pm 1.1$	4.5 ± 1.0
$1 < q^2 < 6$	$1.493 \pm 0.504 \begin{smallmatrix} +0.382 \\ -0.283 \end{smallmatrix}$	$1.8 \pm 0.7 \pm 0.5$	1.60 ± 0.51

Table 1: Measurements of $\mathcal{B}(\bar{B} \rightarrow X_s l^+ l^-)$ [10^{-6}] and their weighted averages for two different ranges of the dilepton invariant mass squared q^2 [GeV^2].

The results in Tab. 1 are averaged over muons and electrons. The first range of the dilepton mass squared q^2 corresponds to the whole available phase-space for $l = \mu$, but includes a cut for $l = e$. Moreover, the intermediate ψ and ψ' are treated as background, and a Monte Carlo simulation based on perturbative calculations is applied for the unmeasured part of the q^2 -spectrum that hides under the huge ψ and ψ' peaks (see Refs. [6, 7] for more details). In the second range of q^2 in Tab. 1, theoretical uncertainties are smaller than in the first case (see below), but the experimental errors are larger due to lower statistics. As we shall see, the analyses in both regions lead to similar conclusions concerning the sign of $A(b \rightarrow s \gamma)$.

The Standard Model perturbative calculations are available at the Next-to-Next-to-Leading Order (NNLO) in QCD for both the considered ranges of q^2 — see Refs. [8, 9] for the most recent phenomenological analyses. The dominant electroweak corrections are also known [8]. In the low- q^2 domain, non-perturbative effects are taken into account in the framework of the Heavy Quark Expansion as Λ^2/m_b^2 and Λ^2/m_c^2 corrections. Analytical expressions for such corrections are also available for the full q^2 range, but they blow up in the vicinity of the intermediate ψ peak. Consequently, a cut needs to be applied, and it is no longer clear what theoretical procedure corresponds to the interpolation that is performed on the experimental side. Thus, the relative theoretical uncertainty for the full q^2 range is larger than for the low- q^2 window.

	Standard Model	$\tilde{C}_7^{\text{eff}} \rightarrow -\tilde{C}_7^{\text{eff}}$
$(2m_\mu)^2 < q^2 < (m_B - m_K)^2$	4.4 ± 0.7	8.8 ± 1.0
$1 < q^2 < 6$	1.57 ± 0.16	3.30 ± 0.25

Table 2: Predictions for $\mathcal{B}(\bar{B} \rightarrow X_s l^+ l^-)$ [10^{-6}] in the Standard Model and with reversed sign of \tilde{C}_7^{eff} for two different ranges of the dilepton invariant mass squared q^2 [GeV^2].

The results of the SM calculations are given in the central column of Tab. 2. For the low- q^2 domain, they correspond to the ones of Ref. [8] with updated input values $m_{t,\text{pole}} = 178.0 \pm 4.3$ GeV [10] and $\mathcal{B}(\bar{B} \rightarrow X_c l \bar{\nu}) = 10.61 \pm 0.16 \pm 0.06$ [11]. The dominant sources of uncertainty are the values of the top and bottom quark masses, as well as the residual renormalization scale dependence. For the full q^2 range, we make use of the statement in Ref. [9] that the NNLO matrix elements for $\hat{s} = q^2/m_b^2 > 0.25$ are accurately reproduced by setting the renormalization scale $\mu_b = m_b/2$ at the Next-to-Leading Order (NLO) level.

The sign of the amplitude $A(b \rightarrow s \gamma)$ is given by the sign of the effective Wilson coefficient \tilde{C}_7^{eff} that determines the strength of the $\bar{s}_L \sigma^{\alpha\beta} b_R F_{\alpha\beta}$ interaction term in the low-energy Hamiltonian. Both the value and the sign of this coefficient matter for the rare semileptonic decay. The results in the right column of Tab. 2 differ from those in the central column only by reversing the sign of \tilde{C}_7^{eff} in the expression for the differential $\bar{B} \rightarrow X_s l^+ l^-$ decay rate¹

$$\begin{aligned} \frac{d\Gamma[\bar{B} \rightarrow X_s l^+ l^-]}{d\hat{s}} &= \frac{G_F^2 m_{b,\text{pole}}^5 |V_{ts}^* V_{tb}|^2}{48\pi^3} \left(\frac{\alpha_{em}}{4\pi}\right)^2 (1 - \hat{s})^2 \left\{ \left(4 + \frac{8}{\hat{s}}\right) |\tilde{C}_7^{\text{eff}}|^2 \right. \\ &\quad \left. + (1 + 2\hat{s}) \left(|\tilde{C}_9^{\text{eff}}|^2 + |\tilde{C}_{10}^{\text{eff}}|^2 \right) + 12 \text{Re} \left(\tilde{C}_7^{\text{eff}} \tilde{C}_9^{\text{eff}*} \right) \right\}, \end{aligned} \quad (1)$$

where \tilde{C}_9^{eff} and $\tilde{C}_{10}^{\text{eff}}$ correspond to the low-energy interaction terms $(\bar{s}_L \gamma_\alpha b_L)(l \gamma^\alpha l)$ and $(\bar{s}_L \gamma_\alpha b_L)(l \gamma^\alpha \gamma_5 l)$, respectively (see Sec. 5 of Ref. [12] for the definitions of all the relevant effective coefficients). The sensitivity of $\mathcal{B}(\bar{B} \rightarrow X_s l^+ l^-)$ to the sign of \tilde{C}_7^{eff} is quite pronounced because the last term in Eq. (1) is sizeable and it interferes destructively (in the SM) with the remaining ones.

One can see that the experimental values of the $\bar{B} \rightarrow X_s l^+ l^-$ branching ratio in Tab. 1 differ from the values in the right column of Tab. 2 by 3σ in both the low- q^2 window and the full q^2 range. This fact disfavors extensions of the SM in which the sign of \tilde{C}_7^{eff} gets reversed while \tilde{C}_9^{eff} and $\tilde{C}_{10}^{\text{eff}}$ receive small non-standard corrections only.

In Fig. 1, we present constraints on additive new physics contributions to $\tilde{C}_{9,10}^{\text{eff}}$ placed by the low- q^2 measurements of $\bar{B} \rightarrow X_s l^+ l^-$ (Tab. 1), once the $\bar{B} \rightarrow X_s \gamma$ bounds on $|\tilde{C}_7^{\text{eff}}|$ are taken into account. Similar plots have been previously presented in Refs. [13, 14]. The two plots correspond to the two possible signs of the coefficient \tilde{C}_7^{eff} . The regions outside the rings are excluded. Surroundings of the origin are magnified in Fig. 2 for the non-standard case. The three lines correspond to three different values of $\mathcal{B}(\bar{B} \rightarrow X_s \gamma) \times 10^4$: 2.82, 3.52 and 4.22, which

¹For simplicity, some of the NNLO QCD, electroweak and non-perturbative corrections are omitted in this expression. However, all those corrections are taken into account in our numerical results and plots.

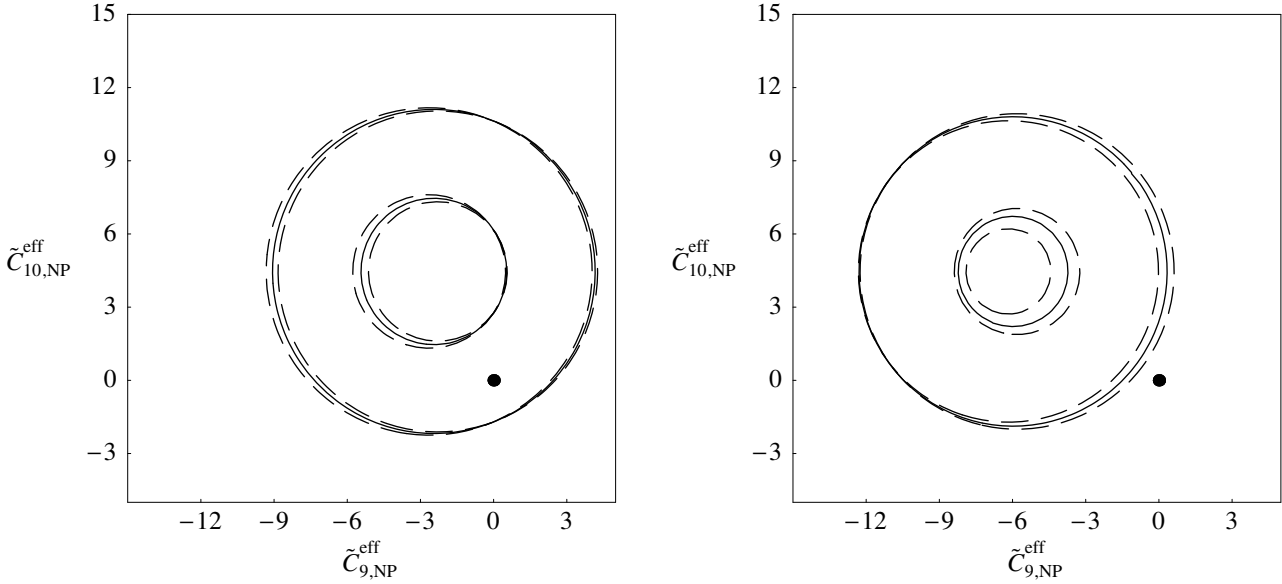


Figure 1: Model-independent constraints on additive new physics contributions to $\tilde{C}_{9,10}^{\text{eff}}$ at 90% C.L. for the SM-like (left plot) and the opposite (right plot) sign of \tilde{C}_7^{eff} . The three lines correspond to three different values of $\mathcal{B}(\bar{B} \rightarrow X_s \gamma)$ (see the text). The regions outside the rings are excluded. The dot at the origin indicates the SM case for $\tilde{C}_{9,10}^{\text{eff}}$.

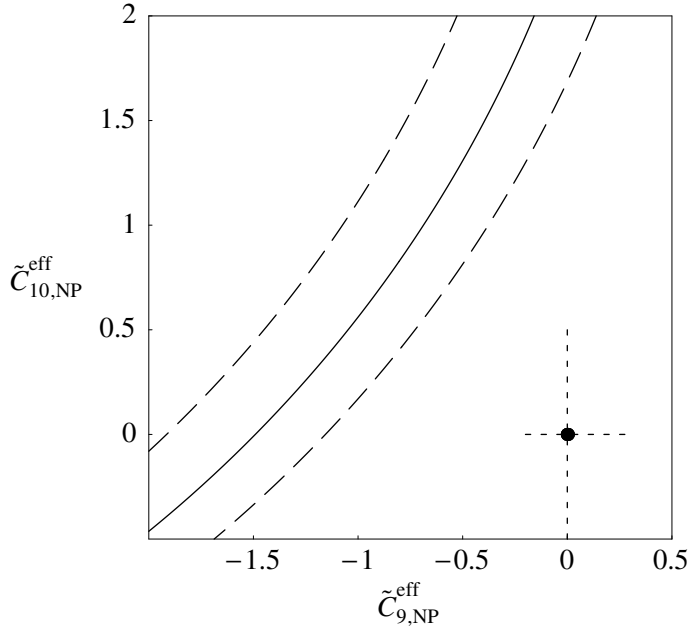


Figure 2: Same as in the right plot in Fig. 1. Surroundings of the origin. The maximal MFV MSSM ranges for $\tilde{C}_{9,\text{NP}}^{\text{eff}}$ and $\tilde{C}_{10,\text{NP}}^{\text{eff}}$ are indicated by the dashed cross (according to Eq. (52) of Ref. [13]).

include the experimental central value as well as borders of the 90% C.L. domain. In evaluating this domain, the experimental error was enlarged by adding the SM theoretical uncertainty in quadrature. A similar procedure was applied to $\mathcal{B}(\bar{B} \rightarrow X_s l^+ l^-)$. Its low- q^2 value was varied between 0.7×10^{-6} and 2.5×10^{-6} .

The SM point (i.e. the origin) is located barely outside the border line of the allowed region in the right plot of Fig. 1. However, one should take into account that the overall scale in this figure is huge, and only a tiny part of the allowed region is relevant to realistic extensions of the SM. Thus, it is more instructive to look at Fig. 2, from which it is evident that a non-standard sign of \tilde{C}_7^{eff} could be made compatible with experiments only by large $\mathcal{O}(1)$ new physics contributions to $\tilde{C}_{9,10}^{\text{eff}}$.²

A case in which large non-standard contributions to \tilde{C}_7^{eff} that interfere destructively with the SM ones arise naturally, while $\tilde{C}_{9,10}^{\text{eff}}$ are only slightly affected, occurs in the Minimal Supersymmetric Standard Model (MSSM) with Minimal Flavor Violation (MFV) at large $\tan \beta$, with relatively light top squark and higgsino-like chargino [3, 13, 15]. The maximal MFV MSSM contributions to $\tilde{C}_{9,10}^{\text{eff}}$ that were found in Ref. [13] are indicated by the dashed cross in Fig. 2. As one can see, they are too small to reach the border of the allowed region.

Configurations of the MSSM couplings and masses for which the sign of \tilde{C}_7^{eff} gets reversed turn out to be relevant if no physics beyond the MSSM contributes to the intergalactic dark matter (see e.g. Ref. [16]). In particular, configurations characterized by large mixing in the stop sector tend to be excluded by the new constraint [17]. While performing a dedicated scan over the MSSM parameters is beyond the scope of the present letter, we expect that the implementation of the $\bar{B} \rightarrow X_s l^+ l^-$ constraints will result in a significant reduction of the neutralino-dark-matter-allowed region in the MSSM parameter space.

One should be aware that in the MSSM at large $\tan \beta$, there are additional contributions suppressed by powers of the lepton masses but enhanced by $(\tan \beta)^3$. They are related to the chirality-flip operators $(\bar{s}_L b_R)(\bar{\mu}_L \mu_R)$ and $(\bar{s}_L b_R)(\bar{\mu}_R \mu_L)$ and may contribute to the muon case in a significant way. Fortunately, such contributions are bounded from above [14, 18] by the experimental constraints [19] on $B_s^0 \rightarrow \mu^+ \mu^-$, and turn out to be irrelevant to our argument.

Another interesting example occurs in the general MSSM with R-parity, where new sources of flavor and CP violation in the squark mass matrices are conveniently parameterized in terms of so-called mass insertions. The sign of the $b \rightarrow s \gamma$ amplitude can be reversed without affecting $\tilde{C}_{9,10}^{\text{eff}}$ if the mass insertion $(\delta_{23}^d)_{LR}$ is large and positive [20]. The new results on $\bar{B} \rightarrow X_s l^+ l^-$ exclude this possibility, and constrain significantly the case of a complex $(\delta_{23}^d)_{LR}$.

To conclude: We have pointed out that the recent measurements of $\mathcal{B}(\bar{B} \rightarrow X_s l^+ l^-)$ by Belle and BaBar already indicate that the sign of the $b \rightarrow s \gamma$ amplitude is unlikely to be different than in the SM. This underscores the importance of $\bar{B} \rightarrow X_s l^+ l^-$ in searches for new physics, and may be relevant for neutralino dark matter analyses within the MSSM.

²The SM values of \tilde{C}_9^{eff} and $\tilde{C}_{10}^{\text{eff}}$ are around +4.2 and -4.4, respectively.

Acknowledgments

We would like to thank I. Blokland, C. Bobeth, S. Davidson, A. Freitas, L. Roszkowski, S. Scopel and L. Silvestrini for helpful discussions and correspondence. M.M. is grateful to INFN Torino for hospitality during his visit. P.G. was supported in part by the EU grant MERG-CT-2004-511156. U. H. was supported by the U.S. Department of Energy under contract No. DE-AC02-76CH03000. M.M. was supported in part by the Polish Committee for Scientific Research under the grant 2 P03B 078 26, and from the European Community's Human Potential Programme under the contract HPRN-CT-2002-00311, EURIDICE.

References

- [1] Heavy Flavor Averaging Group, <http://www.slac.stanford.edu/xorg/hfag>.
- [2] P. Gambino and M. Misiak, Nucl. Phys. B **611** (2001) 338 [hep-ph/0104034];
A. J. Buras, A. Czarnecki, M. Misiak and J. Urban, Nucl. Phys. B **631** (2002) 219 [hep-ph/0203135].
- [3] A. Ali, G. F. Giudice and T. Mannel, Z. Phys. C **67** (1995) 417 [hep-ph/9408213];
P. L. Cho, M. Misiak and D. Wyler, Phys. Rev. D **54** (1996) 3329 [hep-ph/9601360];
J. L. Hewett and J. D. Wells, Phys. Rev. D **55** (1997) 5549 [hep-ph/9610323];
T. Goto, Y. Okada and Y. Shimizu, Phys. Rev. D **58** (1998) 094006 [hep-ph/9804294].
- [4] A. Ali, T. Mannel and T. Morozumi, Phys. Lett. B **273** (1991) 505.
- [5] K. Abe *et al.* (Belle Collaboration), [hep-ex/0410006].
- [6] K. Abe *et al.* (Belle Collaboration), [hep-ex/0408119].
- [7] B. Aubert *et al.* (BABAR Collaboration), Phys. Rev. Lett. **93** (2004) 081802 [hep-ex/0404006].
- [8] C. Bobeth, P. Gambino, M. Gorbahn and U. Haisch, JHEP **0404** (2004) 071 [hep-ph/0312090].
- [9] A. Ghinculov, T. Hurth, G. Isidori and Y. P. Yao, Nucl. Phys. B **685** (2004) 351 [hep-ph/0312128].
- [10] P. Azzi *et al.* (CDF Collaboration), [hep-ex/0404010].
- [11] B. Aubert *et al.* (BABAR Collaboration), Phys. Rev. Lett. **93** (2004) 011803 [hep-ex/0404017].
- [12] H. H. Asatrian, H. M. Asatrian, C. Greub and M. Walker, Phys. Lett. B **507** (2001) 162 [hep-ph/0103087].
- [13] A. Ali, E. Lunghi, C. Greub and G. Hiller, Phys. Rev. D **66** (2002) 034002 [hep-ph/0112300].

- [14] G. Hiller and F. Krüger, Phys. Rev. D **69** (2004) 074020 [hep-ph/0310219].
- [15] C. Bobeth, A. J. Buras and T. Ewerth, [hep-ph/0409293].
- [16] A. Bottino, F. Donato, N. Fornengo and S. Scopel, Phys. Rev. D **69** (2004) 037302 [hep-ph/0307303] and Phys. Rev. D **70** (2004) 015005 [hep-ph/0401186].
- [17] S. Scopel, private communication.
- [18] P. H. Chankowski and L. Ślawianowska, Eur. Phys. J. C **33** (2004) 123 [hep-ph/0308032].
- [19] D. Acosta *et al.* (CDF Collaboration), Phys. Rev. Lett. **93** (2004) 032001 [hep-ex/0403032].
- [20] M. Ciuchini, E. Franco, A. Masiero and L. Silvestrini, Phys. Rev. D **67** (2003) 075016 [Erratum-ibid. D **68** (2003) 079901] [hep-ph/0212397].